https://doi.org/10.2352/AIT.2026.1.1.4

Frequency-dependent capacitance analysis: An empirical equivalent circuit modeling approach to evaluating piezoelectric inkjet printhead actuators

Kazuhide Abe,[1] Mengfei Wong,[2,a)] Ryutaro Kusunoki,[2] Satoshi Kaiho,[2] and Hiroyuki Kushida [2]
[1]Abexyz Inc., Kawasaki, Kanagawa, Japan
[2]RISO Technologies Corporation, Mishima, Shizuoka, Japan

[a)]Author to whom correspondence should be addressed: mengfei_wong@riso.co.jp

Abstract

RISO Technologies, formerly Toshiba Tec's Inkjet Business Unit, continues to provide high-quality shear-mode piezoelectric printhead products to the industrial inkjet printing market since 2001. A non-destructive method has been developed to evaluate piezoelectric actuators by simple LCR measurement. With empirical equivalent circuit modeling, we demonstrate that the approach may provide an insight into the actuator's physical thickness in a finished printhead product and can be used as an alternative method to assess the effectiveness of the precision manufacturing processes by determining dimensional variance.

Introduction

Inkjet printing is a non-contact printing method in which liquid/ink is jetted from tiny, arrayed nozzles in a controlled manner to deposit and form desired texts, images or other information onto a medium. Today, inkjet printing has found applications beyond home and office printing in diverse fields, such as in the signage, labelling/packaging and printed electronics industries.

Among the commercially available printheads adopting different inkjet techniques, shear-mode piezoelectric printhead offers reliable on-demand printing solution with low drive voltages due to its high piezoelectric coefficient (d_{15}). It ejects ink droplet by forcing ink through a nozzle caused by shear deformation of the ink chamber with the application of an electric field across the actuator wall. It does not involve operation that poses mechanical strain on actuators, allowing for long service lifetime with few actuation-related failures.

RISO Technologies, formerly Toshiba Tec's Inkjet Business Unit, started developing shear-mode inkjet printheads in the 1990s under license from Xaar. However, the printhead structure has been evolutionarily revised and differentiated by Toshiba Tec's original technology. Since the launch of Toshiba Tec's inkjet business in 2001, we have continued to provide high-quality shear-mode printheads to the industrial inkjet printing market.

Depends on whether a shear-mode inkjet printhead shares a part of its actuator wall with the adjacent ink chamber, the printhead actuators can be driven in a three-cycle driving mode or a single-cycle driving mode [1]. **Figure 1** shows schematic diagrams of the two driving modes. For a printhead with shared driving walls, such as our CE/CF-series printhead, the actuation of a single ink chamber would greatly affect the neighboring chambers. Therefore, instead of being simultaneously driven, the successive ink chambers are divided into three groups that are sequentially driven in three separate time-division, respectively. On the other hand, for a printhead with the adjacent ink chambers being effectively separated by air chambers, such as our CX1 printhead, the actuation of a single ink chamber would cause only minor crosstalk effect on neighboring chambers. Hence, it is possible to simultaneously drive all ink chambers at the same time. While the single-cycle driving mode's drive frequency is generally thought to be three times higher than that of the three-cycle driving mode, in practice, it is imperative to assign a "restrictor" structure to the printhead in order to achieve stable high-frequency driving.

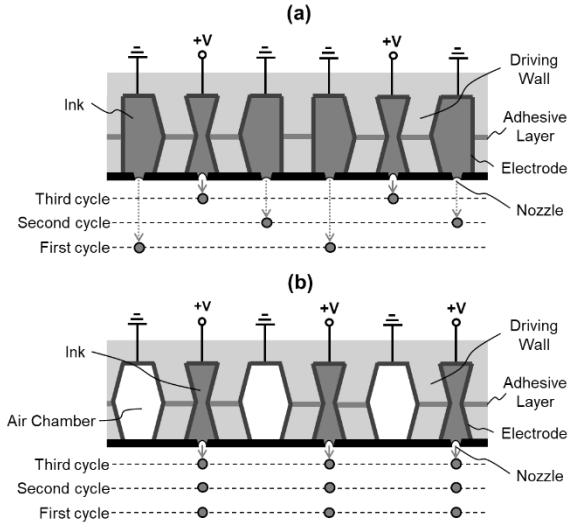

Figure 1. *Illustration of (a) three-cycle driving mode and (b) single-cycle driving mode.*

It has been demonstrated that the flow path that interacts with an actuator in an inkjet printhead can be analogized to an acoustic lumped model consisting of inertance (M), compliance (C), and resistance (R) elements [2]. The mass of the ink flowing through the passage acts as inertance, while the fluid compressibility and the pressure drop caused by viscous loss occurred in the flow path are represented by the compliance and resistance element, respectively. **Figure 2** shows the lumped-element model of the shear-mode single-cycle driven printhead (CX1 printhead), with the assigned "restrictor" structure to achieve stable ink jetting at high frequencies. The three-cycle driving printhead (CE/CF-series) follows the same fundamental model, differing only by the absence of the "restrictor" feature.

The volumetric displacement of the meniscus as a function of time, V(t), can be represented by the following governing equation.

$$\mathrm{M}\frac{\mathrm{d}^2\mathrm{V(t)}}{\mathrm{dt}^2} + \mathrm{R}\frac{\mathrm{dV(t)}}{\mathrm{dt}} + \frac{1}{\mathrm{C}}\cdot\mathrm{V(t)} = 0 \qquad (1)$$

By defining parameter γ and ω as a function of inertance (M), compliance (C) and resistance (R), Equation (1) can be rewritten as

$$\frac{d^2V(t)}{dt^2} + 2\gamma\frac{dV(t)}{dt} + \omega^2 \cdot V(t) = 0\,, \qquad (2)$$

where $\gamma = \frac{R}{2M}$ and $\omega = \sqrt{\frac{1}{CM}}$.

The solution to Equation (2) can then be expressed as

$$V(t) = Ae^{\left(-\gamma+\sqrt{\gamma^2-\omega^2}\right)t} + Be^{\left(-\gamma-\sqrt{\gamma^2-\omega^2}\right)t}\,, \qquad (3)$$

where A and B are arbitrary constants.

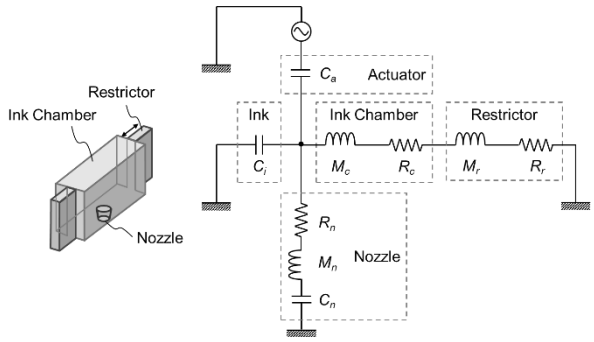

Figure 2. *Lumped-element model of the shear-mode single-cycle driven printhead (image not to scale). The subscript a, i, c, n and r denote actuator, ink, ink chamber, nozzle and restrictor, respectively. The shear-mode three-cycle driving printhead follows the same model without the "restrictor" feature.*

Figure 3 shows the change in volumetric displacement of meniscus following an ink jetting operation based on Equation (3). In the case of $\gamma^2 - \omega^2 < 0$, for example $\gamma^2/\omega^2 = 0.1$, the meniscus is in underdamped condition. It overshoots following an ink jetting operation and oscillates for some time before subduing. On the other hand, if $\gamma^2 - \omega^2 > 0$ or $\gamma^2/\omega^2 > 1$, the meniscus displacement is in overdamped condition. While in this case the meniscus does not overshoot following an ink jetting operation, it takes longer time to restore to its original position. Consequently, we estimate that a shear-mode actuator shall ideally have dimensions with overall inertance, compliance and resistance satisfying $0.2 \le \gamma^2/\omega^2 \le 1.0$, i.e., $0.2 \le (R^2C/4M) \le 1.0$ [3].

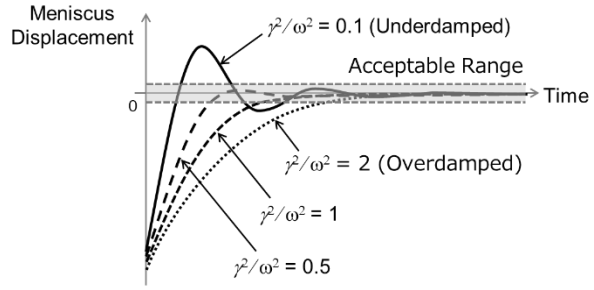

Figure 3. *Estimate of meniscus restoration movement following an ink jetting operation with varying γ^2/ω^2.*

Figure 4 shows an example of ink jetting image using CX1 printhead, manufactured with design dimensions based upon the above estimate finding. With adequate waveform tuning and temperature control, it has been demonstrated that ink droplets can be stably jetted at high frequencies.

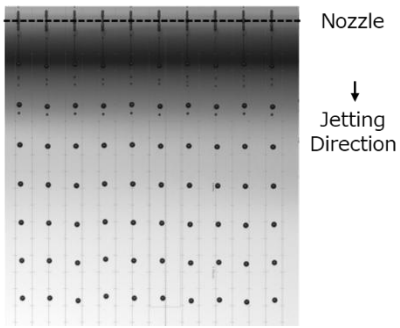

Figure 4. *Images of oil-based ink jetting using a shear-mode single-cycle driven printhead (CX1 printhead) driven at 35 kHz at a jetting viscosity of approximately 7 mPa·s.*

While precision manufacturing processes are critical for achieving the desirable dimensions needed for high yield and inkjet performance, the current final-product evaluation methods, such as ink droplet observation or test-printed results, complicate the assessment. These tests involve complex ink-printhead interactions, which may obscure the assessment of true actuator performance. Furthermore, if an ink jetting issue occurs, confirming the actuator's condition without resorting to destructive microscopic inspection remains elusive.

Here we present a study on the frequency-dependent capacitance of the shear-mode piezoelectric actuators to provide an alternate insight into the actuator's physical wall thickness in a finished printhead product. It is aimed to assess the effectiveness of the precision manufacturing processes by determining dimensional variance, or to troubleshoot the actuators, in case of any issues, without damaging the inspected pieces.

Experimental Procedure

The capacitance and impedance/admittance responses of shear-mode piezoelectric printhead actuators (RISO Technologies' single-cycle driven CX1 printhead actuators), between 20 Hz and 1 MHz, were measured using a precision LCR meter (HP 4284A), supported by an interface control program written using Microsoft Excel's Visual Basic for Application (VBA). Those data below 100 Hz were omitted due to utility interference effect caused by the local power line. The data were then fitted based on modeled equivalent circuits using LTspice simulation software. For comparison purposes, the test pieces included actuators with and without surface treatment, and a reference mica capacitor. The surface treatment was aimed to modify the surface of the actuator's driving walls in order to improve electrode's adhesion.

Results

Figure 5 shows graphs of the measured capacitance value against voltage frequency for a CX1 printhead actuator (without surface treatment) and a reference mica capacitor with a nominal capacitance value of C_{ref}. The measurement results are obtained by applying an ac bias with a Vrms value of 0.3V on top of a dc bias varied in a sequential order of 0V ($0V_{ini}$), +10V, 0V ($0V_{mid}$), -10V and 0V ($0V_{end}$). As shown in **Figure 5(a)**, the measured capacitance results of the CX1 printhead actuator with various dc biases overlap and do not significantly differ from each other, indicating minimal dc bias effects toward changes in dielectric properties. Below 100 Hz, the capacitance considerably fluctuates due to utility interference effect caused by the local

power line at 50 Hz. Beyond 100 kHz, on the other hand, the capacitance dramatically decreases when the noise interference effect caused by the measuring coaxial cable becomes dominant. Similar results can be observed for the mica capacitor, as shown in **Figure 5(b)**, except that between 100 Hz and 100 kHz, the capacitance of the CX1 printhead actuators linearly decreases with the voltage frequency on a log scale, while that of the reference mica capacitor shows a constant trend.

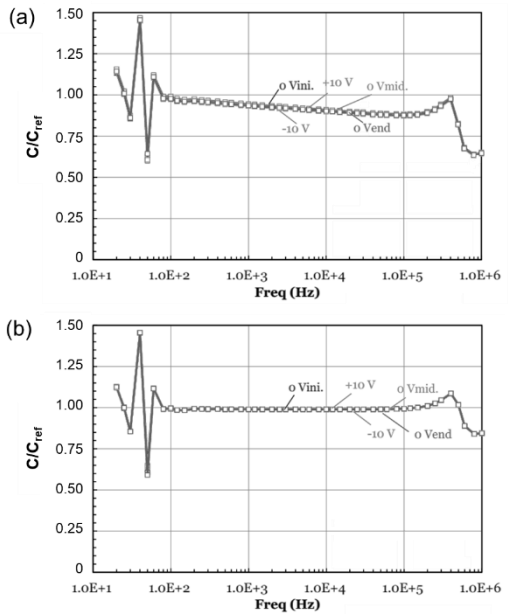

Figure 5. *Frequency-dependent capacitance measured by varying dc bias for (a) a CX1 printhead actuator (without surface treatment) and (b) a mica capacitor with a nominal capacitance value of C_{ref}.*

As the piezoelectric printhead actuator exhibits behavior different from a pure capacitor, two preliminary equivalent circuit models, as demonstrated in **Figure 6**, are proposed to further analyze the capacitance results. **Figure 6(a)** shows the simpler Model 1 whereby the actuator is represented by a single capacitance element, while **Figure 6(b)** shows the more complicated Model 2 consisting of a capacitor and a series of five parallel RC circuits with different degrees of cut-off frequency ranging from to 1 Hz to 10 kHz, namely 1 Hz, 10 Hz, 100 Hz, 1 kHz and 10 kHz. Model 2 assumes that the actuator contains five equal-thickness layers with the same capacitance value ($C_n = C_1 = C_2 = \ldots = C_5$), that is less electrically insulated than the interior part (C_0). The cut-off frequency, f_n can be related to C_n and R_n by the following equation.

$$f_n = \frac{1}{2\pi C_n R_n} \tag{4}$$

For initial model validation purposes, the value of C_n is obtained based on the following assumption.

$$\frac{3}{C_n} = \frac{1}{C_{100kHz}} - \frac{1}{C_{100Hz}} \tag{5}$$

Both Model 1 and 2 contain RLC elements corresponding to the coaxial cable.

Figure 7 presents the data fitting results of the two proposed models. By omitting the data below 100 Hz, Model 2 shows better fitted results compared with Model 1. Similar conclusion is drawn from data fitting of admittance and phase angle values (not shown). The result suggests that the printhead actuator structure may resemble that comprising multiple thinner layers with gradually different properties from the interior part. While researchers have reported the existence of surface layer in millimeter and sub-millimeter bulk ceramic materials, there is still a limited understanding of the underlying mechanisms, considering factors such as the random field effect associated with surface charge carriers, differences in lattice parameters between the surface and bulk material, and variations in polarization states from the surface to the bulk [4,5].

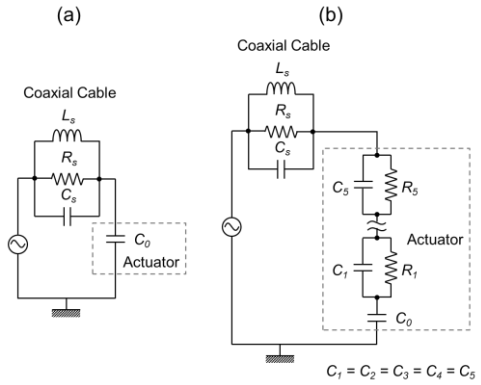

Figure 6. *Equivalent circuit model for the CX1 printhead actuator: (a) Model 1 and (b) Model 2.*

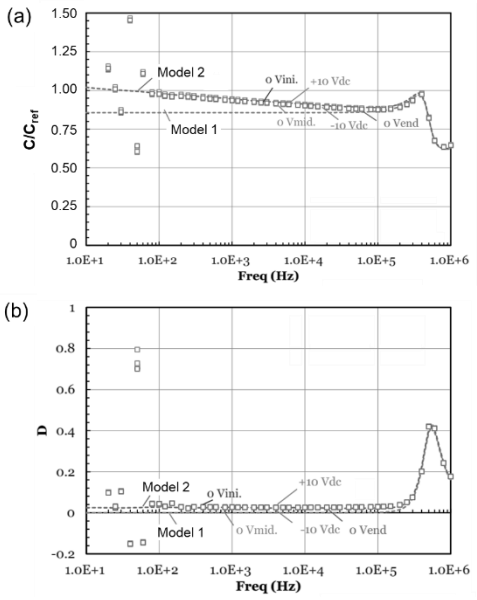

Figure 7. *Data fitting results based on equivalent circuit models shown in Figure 6: (a) Capacitance and (b) Dielectric loss.*

We then refine Model 2 by extending the actuator's layers to nine layers with a cut-off frequency ranging from to 1 Hz to 100 MHz, namely 1 Hz, 10 Hz, 100 Hz, 1 kHz, 10 kHz, 100 kHz, 1 MHz, 10 MHz and 100 MHz. The revised empirical equivalent circuit model, together with the actuator's physical interpretation is presented as Model 3 in **Figure 8**. Unlike Model 2, these layers are assumed to have different capacitances and, hence, different thicknesses, considering that capacitance decreases with cut-off frequency, as shown in **Figure 5(a)**.

It should be noted that while the capacitance value does not change with the dc bias, it increases with the ac bias (Vrms) across the tested range from 0.3V to 10V. When plotting capacitance against frequency on a log scale, both the graph's

slope and intercept linearly increase with the ac bias, as shown in **Figure 9(a)** to **9(c)**. Based on these relationships, the capacitance response to varying ac bias can be predicted without actually performing the test. This predicted response is illustrated by the dotted Vrms lines of 15V, 20V and 25V in **Figure 9(a)**.

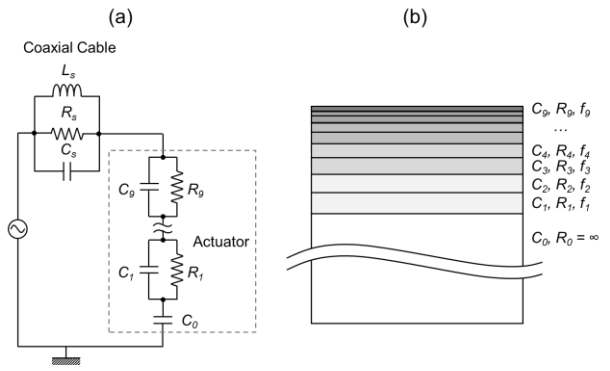

Figure 8. *(a) Refined equivalent circuit model (Model 3) for the CX1 printhead actuator and (b) its physical interpretation.*

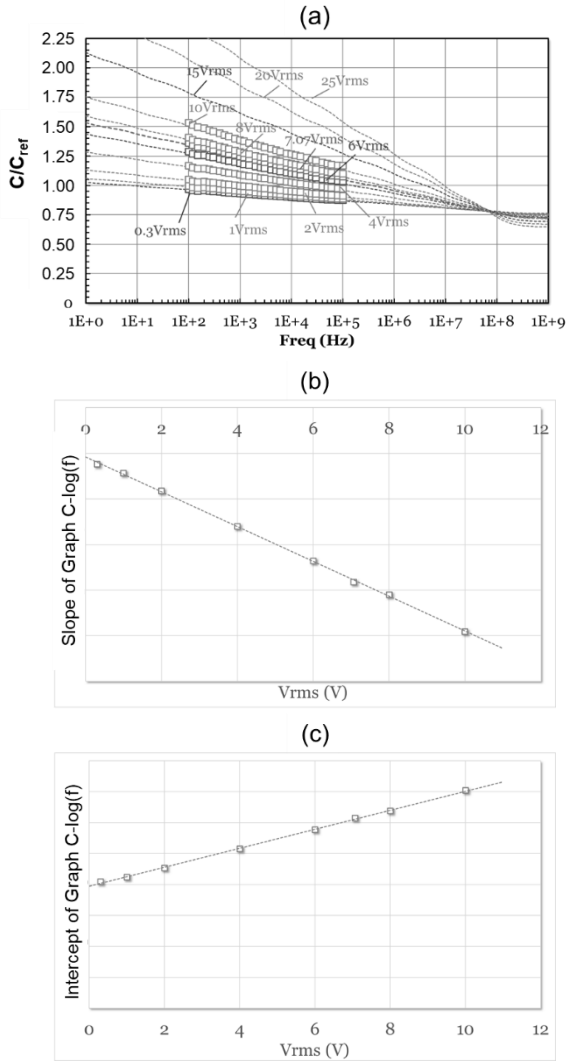

Figure 9. *(a) Capacitance response of the CX1 printhead actuator by varying ac bias (Vrms), showing that (b) the graph's slope and (c) intercept linearly increase with the ac bias.*

By extrapolating the capacitance data points, the capacitance responses are found to converge at a high frequency point around 100 MHz (f_x). Using the capacitance value of this convergent point (C_x), an "effective" thickness that may reflect the physical thickness of the actuators can be calculated according to the following equation.

$$d_x = \frac{\epsilon_0 \epsilon_r A}{C_x} \quad (6)$$

where A is the design value of the electrode's area. The electrical resistivity can also be obtained by using the following equation.

$$\rho_x = \frac{1}{2\pi\epsilon_0 \epsilon_r f_x} \quad (7)$$

where ρ_x is the electrical resistivity at the convergent frequency (f_x), ε_r is the relative permittivity and ε_0 is the vacuum permittivity.

Table 1 shows the "effective" thickness relative to its design value (d_0) and the actuator's electrical resistivity calculated using equation (6) and (7), respectively. The actuators with and without surface treatment show an expected result whereby a few micrometers difference exists in the "effective" thickness. This suggests that the equivalent circuit modeling approach in this study can be used as an alternative method to assess the actuator's physical thickness in a finished printhead product as well as to evaluate the effectiveness of the precision manufacturing processes by determining dimensional variance in a non-destructive manner.

On the other hand, the resistivity, in the order of 10^{-2} Ω·m, is significantly lower than what we expect for a dielectric or an insulator, in the range of 10^8 to 10^{12} Ω·m. This may be related to scaling or surface effects in other findings, suggesting that as the thickness of the ceramics decreases, notable reductions in both the piezoelectric response and permittivity occur [4,5]. The detailed investigation, however, is beyond the scope of this study.

Table 1: "Effective" thickness and electrical resistivity of CX1 printhead actuator

Condition	C_x/C_{ref}	f_x	d_x/d_0	ρ_x
Without surface treatment	0.78	103 MHz	1.07	7.2×10^{-2} Ω·m
With surface treatment (Process 1)	0.87	121 MHz	0.95	6.1×10^{-2} Ω·m
With surface treatment (Process 2)	0.90	229 MHz	0.92	3.2×10^{-2} Ω·m

Conclusions

Based on empirical frequency-dependent capacitance analysis, equivalent circuit models consisting of a capacitor and a series of multiple parallel RC circuits with different degrees of cut-off frequency are proposed to evaluate piezoelectric actuators by simple LCR measurement. The analysis result suggests that our shear-mode printhead actuators, or to a greater extent, sub-millimeter order piezoelectric actuators, may have a structure resembling that comprising multiple thinner layers with gradually different properties from the interior part. The analysis may be used to determine dimensional variance of a finished printhead product, or to troubleshoot the actuators in a non-destructive manner.

References

[1] A. Tomotake, Technology of Konica Minolta's Inkjet Printhead, in Inkjet Printing in Industry, Vol. 1 (Wiley-VCH, Weinheim, Germany, 2022) pg. 508.

[2] S. Sakai, "Fine Droplets Technology of Piezoelectric Inkjet Printhead", J. Imaging Soc. Japan, 40, 1, 48 (2001).

[3] Japanese Laid-Open Patent Publication No. 2004-168045.

[4] J. Jia et al., "Impact of oxygen vacancy-gradient surface layer on the electrostrain of Sb^{3+} doped BNKST ceramics," Appl. Phys. Lett., 126, 202901 (2025).

[5] Tian et al., "Thickness dependence of dielectric and piezoelectric properties from the surface layer effect of $BaTiO_3$-based ceramics," Ceram. Int., 47(12), 17262 (2021).

Author Biography

Kazuhide Abe received his B. Eng. and M. Eng. degrees in physical electronics from the Tokyo Institute of Technology in 1982 and 1984, respectively. He was a Senior Research Scientist at the Corporate Research and Development Center of Toshiba Corporation before founding Abexyz Inc. as a technical consultant. His research interests cover dielectric, ferroelectric and piezoelectric thin films as well as their applications including radio-frequency devices and circuits. He was designated as a Fellow of the Japan Society of Applied Physics (JSAP) in 2010.

Mengfei Wong is a group manager and project leader of the Inkjet Printhead Development Department at RISO Technologies Corporation. He has over 10 years of working experience in the field of printhead development and is co-inventor on 15 patent families in the piezoelectric/inkjet domain. He obtained his B.Eng. degree in mechanical engineering from the University of Technology Malaysia (2005) and his Ph.D. degree from the National University of Singapore (2011).

Ryutaro Kusunoki received his B.Eng. degree from the Tokyo University of Science in 1989 and joined Tokyo Electric Co., Ltd. (now Toshiba Tec Corporation) in the same year. He has been involving in the research and development of inkjet printhead since 1993, contributing to over 90 Japanese patents. His research interests include piezoelectric inkjet printhead design, simulation and ink jetting evaluation.

Satoshi Kaiho is the General Manager of the Inkjet Printhead Development Department at RISO Technologies Corporation. He joined Toshiba Corporation in 1992 as a product development engineer, before moving to Toshiba Tec Corporation in 2001. He has held various managing roles in different departments since 2011. He received his B.Eng. degree from Waseda University (1992) and his master's degree in management of technology (MOT) from the Tokyo University of Science (2008).

Hiroyuki Kushida is the Technology Executive of the Inkjet Business Division at RISO Technologies Corporation. He received his B.Sc. degree from the Tokyo University of Science (1989) and joined Tokyo Electric Co., Ltd. (now Toshiba Tec Corporation) in the same year. He is a member of the Japan Society of Applied Physics (JSAP) and the Imaging Society of Japan (ISJ).